IEEE Access
Multidisciplinary | Rapid Review | Open Access Journal

Received 15 February 2024, accepted 4 April 2024, date of publication 8 April 2024, date of current version 17 April 2024.

Digital Object Identifier 10.1109/ACCESS.2024.3386367

RESEARCH ARTICLE

Classification of Hand-Movement Disabilities in Parkinson's Disease Using a Motion-Capture Device and Machine Learning

JUNGPIL SHIN[1], (Senior Member, IEEE), MASAHIRO MATSUMOTO[1], MD. MANIRUZZAMAN[1], MD. AL MEHEDI HASAN[2], (Member, IEEE), KOKI HIROOKA[1], (Graduate Student Member, IEEE), YUKI HAGIHARA[3], NAOKI KOTSUKI[4], SATOMI INOMATA-TERADA[5], YASUO TERAO[5], AND SHUNSUKE KOBAYASHI[3]

[1]School of Computer Science and Engineering, The University of Aizu, Aizuwakamatsu 965-8580, Japan
[2]Department of Computer Science and Engineering, Rajshahi University of Engineering and Technology, Rajshahi 6204, Bangladesh
[3]Department of Neurology, Teikyo University, Tokyo 173-8605, Japan
[4]Department of Neurology, Kyorin University, Tokyo 181-8611, Japan
[5]Department of Medical Physiology, Kyorin University, Tokyo 181-8611, Japan

Corresponding authors: Jungpil Shin (jpshin@u-aizu.ac.jp) and Shunsuke Kobayashi (skoba1230@gmail.com)

This work was supported by Japan Society for the Promotion of Science (JSPS) Grants-in-Aid for Scientific Research (KAKENHI), Japan, under Grant JP20H04493.

This work involved human subjects or animals in its research. Approval of all ethical and experimental procedures and protocols was granted by the Ethics Review Committees of Teikyo University Hospital and Kyorin University Hospital under Application No. Teirin20-279 and R03-014, respectively and performed in line with the Declaration of Helsinki.

ABSTRACT Parkinson's disease (PD) is a neurological disorder caused by degeneration of dopaminergic neurons in the midbrain. PD patients mainly suffer from motor symptoms, which significantly impact their daily lives. The diagnostic criteria for PD include the presence of muscle rigidity, tremor, and postural reflex disturbances. The Movement Disorder Society Unified Parkinson's Disease Rating Scale (MDS-UPDRS) is the standard tool for evaluating PD symptoms, part III of which is dedicated to motor symptoms. That part involves a comprehensive set of specific physical examinations, and physicians assign semi quantitative scores from 0 to 4. However, this approach faces notable challenges, including the requirement for movement-disorder experts proficient in using MDS-UPDRS and the presence of substantial inter rater variability even among experts. Overcoming these challenges requires a quantitative and objective assessment method. Given that the rating of motor symptoms predominantly involves assessing kinematic characteristics, the integration of sensor-based devices and machine learning techniques holds the potential to outperform human experts in symptom evaluations. This study used the Leap Motion optical motion-capture device to quantitatively measure and analyze hand movements while 45 PD patients performed the following 3 tasks from the MDS-UPDRS part III: finger tapping (FT), hand opening and closing (OC), and forearm pronation and supination (PS). Data from these tasks were collected and processed, resulting in the extraction of 31 movement patterns for each task. Additionally, 69 statistical features were extracted from each movement pattern, yielding 2139 features for each task. We subsequently employed a random forest algorithm to select the top 15% of features based on the reduction of Gini impurity. These selected features were subsequently fed into a sequential-forward-floating-selection algorithm, combined with a support vector machine, to identify relevant feature combinations and predict the severity of the motor symptoms. The classification accuracy was 87.0% for FT, 93.2% for OC, and 92.2% for PS. One-way analysis of variance identified 13 features of the OC task that were significantly more discriminative for classifying the movement disability of PD patients (p<0.05). This study highlights the effectiveness of combining sensor-based measurements with machine learning for symptom assessment, which demonstrated performance

The associate editor coordinating the review of this manuscript and approving it for publication was Xinyu Du.

comparable to that of expert physicians. Implementing these findings in clinical settings holds the promise of applying objective and quantitative methods for evaluating the symptoms of PD and related disorders.

INDEX TERMS Classification, Parkinson's disease, MDS-UPDRS, leap motion, machine learning.

I. INTRODUCTION

Parkinson's disease (PD) is the second-most-prevalent neurodegenerative disorder. PD is caused by the degeneration of midbrain dopaminergic neurons and the accumulation of Lewy bodies composed of abnormal synuclein within the brain [1]. PD patients suffer from a diverse array of symptoms that profoundly impair both motor and nonmotor facets of their daily lives [2]. The hallmark clinical triad of akinesia, rigidity, and tremor is the key for diagnosing parkinsonism [1], [3]. The severity of these clinical features may change during the natural course of the disease, in response to treatment, or even fluctuate within a single day due to long-term motor complications. Therefore, the availability of quantitative assessments of motor symptoms is highly important for diagnosis and evaluative purposes. It is crucial that sensitive and specific measures of motor symptoms are applied to effectively reflect the impact of treatments, especially in the context of clinical trials.

Various methods have been developed to assess PD symptoms, including Hoehn-Yahr staging, the Schwab and England Scale [4], and the Unified Parkinson's Disease Rating Scale (UPDRS). In 2008, the Movement Disorders Society (MDS) revised the UPDRS to produce the MDS-UPDRS, which has become the standard tool [5]. The MDS-UPDRS consists of four parts, with part III dedicated to motor symptoms employing a comprehensive list of specific physical examinations, with physicians assigning semiquantitative scores ranging from 0 to 4, where 0 indicates a normal finding and a higher score indicates greater severity. Akinesia is evaluated by measuring the speed, amplitude, and rhythm of repetitive movements during finger tapping (FT), hand opening and closing (OC), and forearm pronation and supination (PS).

However, there are several limitations in the current rating-scale approach: It requires experts who are well-trained in the use of the MDS-UPDRS. Although interrater reliability is high among adequately trained examiners, some interrater variability persists [6]. Sensor-based devices designed for quantitative kinematic measurements of limb movements have recently become readily available. These devices include wearable sensors [7], [8], [9], accelerometers [10], gyroscopes [11] and camera-based sensors [12], [13], [14], but they might not be suitable for practical application in clinical settings due to their size, cost, and time requirements. In addition, although video recording devices are inexpensive, they mostly are not able to capture small finger movements [14].

To address these challenges, we utilized an optical motion-capture device as a novel and promising solution for recording hand movements in PD patients [15]. This so-called Leap Motion device (LMD) has several key advantages over other wearable devices, including compact size, affordability, high-resolution image acquisition, and minimal need for markers or devices on subjects during data collection. These attributes render the LMD well suited for the quantitative assessment of motor symptoms in PD patients. On the other hand, the LMD also has certain limitations [16]. For example, it is difficult to detect whole-body movements, which is important since PD symptoms such as akinesia, rigidity, and tremor affect the legs, posture, and gait [16]. It is also difficult to evaluate rigidity using the LMD since this does not directly relate to kinematics. In this study we evaluated akinesia using the FT, OC, and PS tasks in the MDS-UPDRS part III.

Machine learning (ML)-based algorithms are becoming increasingly prominent in various healthcare sectors [17], [18], [19], [20], [21], [22], serving purposes such as supporting clinical diagnosis, classifying disease stages, and predicting clinical outcomes [23], [24]. ML-based methods have emerged as robust approaches for identifying complex data patterns, automating data analysis, and making inferences/classifications related to diseases, including PD [25], [26]. Furthermore, ML enables computer programs to learn and extract meaningful features from data that are not conventionally used in the clinical diagnosis of PD. The performance of ML-based algorithms is highly dependent on input features. Meaningful input features are extracted from abundant generated sensor data through the application of statistical tests and feature-selection techniques. Nowadays, sequential forward floating selection (SFFS) and random forest (RF) have been widely used to select relevant combinations of features over different fields [27], [28]. In this study we also used SFFS to determine the combinations of potential features for PD patients. These selected potential features were then included in ML-based algorithms to classify stages of hand-movement disabilities in PD. Previous studies have utilized various ML-based algorithms to detect neurodegenerative diseases, including support vector machines (SVMs), deep learning (DL), and neural networks [29], [30]. In particular, SVMs have been widely used in healthcare due to their superior performance relative to traditional methods [31], [32]. SVMs have a low risk of over-fitting and can build relatively robust models for unknown data. In addition, SVMs have the flexibility to accommodate both linear and nonlinear classification. The motor symptoms of PD have linear or nonlinear features depending on the severity. Therefore, SVMs can accommodate a wide variety of data and we used an SVM to evaluate the hand movements of PD patients. In summary, this study performed the following tasks:

- Collecting hand gesture signals using the LMD while performing FT, OC, and PS tasks.
- Computing the movement patterns for each task.
- Extracting statistical features from each movement pattern.
- Adapting an RF-based algorithm to sort the features based on the reduction of Gini impurity and select the top 15% of features.
- Implementing SFFS with an SVM to determine the combination of relevant features based on the classification accuracy.
- Performing the statistical validations of the selected features using a p-value criterion of <0.05.

The remainder of this paper is organized as follows: Section II reports on related work. Section III describes the proposed methodology, data-collection device, participant selection, motor tasks, data acquisition, data preprocessing, movement-patterns analysis, extreme-value detection, feature extraction, and feature selection using RF and SFFS, and statistical validations are also described in this section. Section IV presents the experimental setup and performance metrics. The experimental results and discussion are presented in Section V. Finally, the conclusion, limitation, and future work are presented in Section VI.

II. RELATED WORK

In clinical practice, neurological symptoms are assessed through physical examinations. The examinations performed for movement disorders such as PD mostly involve assessing the kinematic features of various types of movement. This has been implemented using sensor-based devices to capture PD symptoms, such as Chen et al. [33] developed the objective and interpretable PD-Net visual system based on video images obtained from the OpenPose library. Their system comprised three modules: (i) a pose detector capable of identifying 21 key locations on the hand in RGB video recording, (ii) an analysis of task motor patterns based on key locations on the hand and the identification of motor signs, and (iii) a scoring module for predicting MDS-UPDRS scores based on identified symptoms. Using hand-gesture signals from 149 PD patients performing FT, OC, and PS tasks, Chen et al. demonstrated that the PD-Net system achieved an accuracy of 87.6% and a Cohen's kappa coefficient of 0.82. However, it should be noted that because their system relies on a monocular camera, its three-dimensional (3D) spatial recognition capabilities are inferior to those of systems based on the LMD.

Guo et al. [34] similarly devised a novel computer-vision-based system for detecting PD symptoms. They used a depth camera and 3D hand pose estimation, collecting 112 videos of 59 subjects (48 with PD and 11 controls) performing the FT task. Various motion-based features, including amplitude, velocity, and rhythm, were computed using the tsfresh package in Python [35]. They selected the most effective features based on correlation coefficients and included them in ML models to identify PD patients. Multiple ML-based models, including k-nearest neighbors, RF, extreme gradient boosting, and SVMs with linear and radial basis function (RBF) kernels were evaluated for their usefulness in predicting a PD diagnosis. The highest classification accuracy of 81.2% was achieved using an SVM with an RBF kernel. Dadashzadeh et al. [36] proposed an end-to-end DL-based framework for assessing the severity of PD symptoms based on the patient's gait and ability to perform hand-movement tasks. To evaluate the performance of their proposed system, they collected a data set of 1058 videos from 25 PD patients. Their algorithm achieved a highest classification accuracy of 77.1% for gait and 72.3% for hand movements.

Butt et al. [37] similarly developed an ML-based system using the LMD to distinguish PD patients from healthy controls. They collected hand gesture signals from 28 subjects, which including 16 PD patients. Data were acquired while the subjects performed FT, OC, and PS tasks, and during the presence of postural tremor. Various time-domain and frequency-domain features including angle, velocity, amplitude, and frequency were extracted from the raw data sets. Feature selection was subsequently performed using correlation coefficients, followed by ML-based algorithms such as logistic regression, naive Bayes (NB), and an SVM trained to identify PD patients. The NB algorithm achieved the highest average accuracy of 81.4%.

III. MATERIALS AND METHODS

A. PROPOSED METHODOLOGY

The overall experimental workflow employed in this study is presented in Fig. 1. We used the LMD to evaluate akinesia in the hands of PD patients while they performed three hand-related tasks from the MDS-UPDRS part III (FT, OC, and PS). The study was conducted by following a series of five key steps. The first step involved data preprocessing, in which we eliminated redundant variables and standardized the data frame rate. Additionally, we computed 31 distinct movement patterns for the FT, OC, and PS tasks. The second step encompassed feature extraction. In this step, we identified extreme values and extracted 69 features from each of the computed movement pattern. Following feature extraction, we used an RF classifier to measure the Gini impurity for feature importance of each task, and then arranged arranged the value of Gini impurity in descending order. We selected the top 15% of features based on their Gini impurity scores, which were used in SFFS to identify the most-relevant combinations. The chosen feature set was employed to train an SVM model, which underwent hyperparameter tuning. Using the Optuna framework, we effectively optimized three SVM parameters: kernel function, cost and gamma (γ). The optimization process was repeated 200 times with the seed value set to 42. We selected the optimal parameter values that provided the highest classification accuracy. After optimizing the hyperparameters, the SVM model was trained using leave-one-out cross-validation (LOOCV) and then used to

predict the disease severity of the PD patients, before classifying them into five categories: normal, slight, mild, moderate, and severe. The performance of the SVM model was evaluated using performance metrics such as classification accuracy, recall, precision, and F1-score.

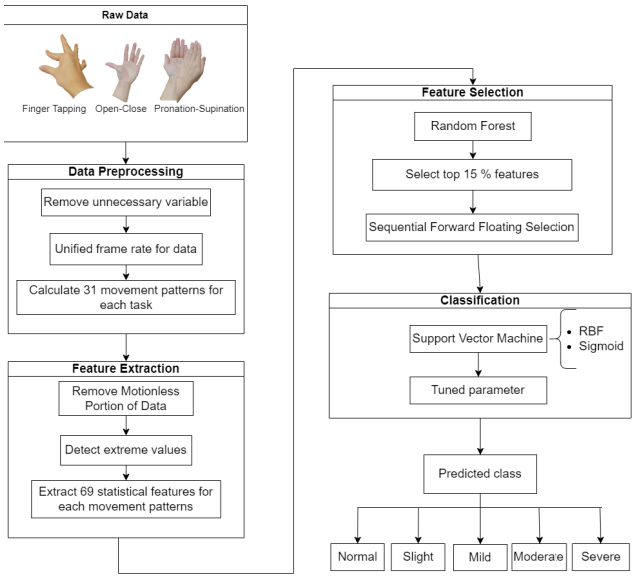

FIGURE 1. Flowchart of the proposed ML-based method for predicting PD patients.

B. DATA COLLECTION DEVICE

An LMD was used to collect data. This is a noncontact optical device manufactured by Ultraleap (CA, USA) and equipped with two infrared cameras and three infrared LEDs. This device facilitates the capturing of hand motion and position in three dimensions. The LMD operates within a right-handed coordinate system, as illustrated in Fig. 2, where the y-axis signifies depth toward the sensor, the z-axis ascends towards the user, and the x-axis extends to the right [38], [39]. Its field of view is 150 degrees x 120 degrees.

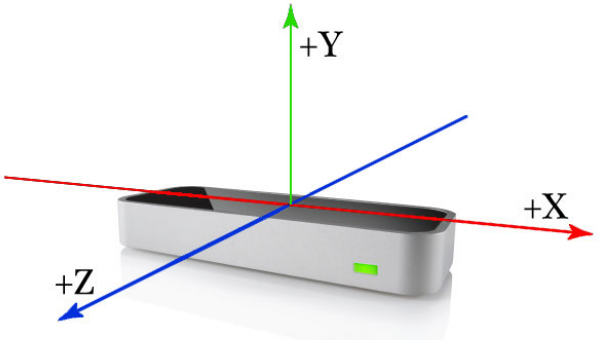

FIGURE 2. Leap motion device coordinate system.

The region where the user's hand or fingers interact with the LMD's field of view is referred to as the interaction box [40]. Within this box, the y-axis spans from 82.5 mm to 317.5 mm above the device, while the x-axis ranges from 117.5 mm to -117.5 mm, and the z-axis extends from 73.5 mm to -73.5 mm [40] However, the tracking accuracy is contingent on factors such as hand-camera distance, lighting conditions, and the specific part of the hand being tracked. Vysocky et al. [41] demonstrated that the detected position deviates from the actual position by no more than approximately 5 mm within the interaction box. Beyond this boundary, errors could reach up to 10 mm, with measurements remaining stable both inside and outside the box [41]. The LMD is cost-effective, compact, and easy to use. It has dimensions of 80 mm x 30 mm x 11 mm and weighs 45 g, and interfaces with computers via USB to instantly and accurately display hand movements on the screen. Remarkably, the operation of the LMD is not affected by environmental conditions, instead being solely dependent on hand-based information.

Fig. 3 shows the anatomical arrangement of each finger encompassing four bones: the metacarpal, proximal phalange, intermediate phalange, and distal phalange [42]. It is noteworthy that the thumb lacks an intermediate phalange. The LMD identifies fingers based on their fingertips, while the length of the metacarpals is set to zero [42]. The LMD supplies time-series data, including finger joint positions and the orientation of the palm. In this study we used software compatible with two different versions of the LMD API: versions 3.2 and 4.1.0. We ensured data consistency by harmonizing the format of version 3 with that of version 4. Although some variables were missing due to version disparities, they were deemed nonessential for achieving the objectives of this study.

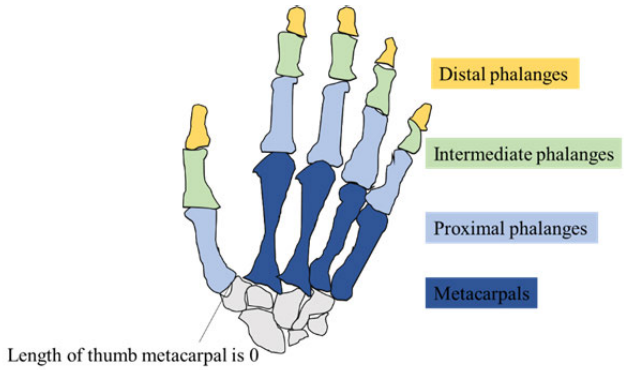

FIGURE 3. Four bones constituting each finger.

C. PARTICIPANT SELECTION

Participants for inclusion in this study were recruited from two esteemed medical institutions: Teikyo University Hospital and Kyorin University Hospital. All participants had been diagnosed as PD by board-certified neurologists with expertise in movement disorders (N.K., S.I.T., Y.T., and S.K.) following the diagnostic criteria established by the MDS [3]. Our cohort consisted of 45 PD patients whose ages range from 49 years to 87 years. Prior to participating in the study, all individuals provided written informed consents.

All of the study procedures were approved by the ethics review committees of Teikyo University Hospital and Kyorin University Hospital (approval ID numbers Teirin20-279 and R03-014, respectively).

D. MOTOR TASKS

Each participant was instructed to perform three distinct motor tasks selected from the MSD-UPDRS: FT, OC, and PS. Before recording data, an examiner demonstrated how to perform each task, and the participants were given the opportunity to practice them. The start of each measurement session was signaled by a tone. We recorded each task multiple times for both the left and right hands to ensure comprehensive and accurate data collection. To accurately track the hand movements, participants positioned their palms facing the LMD sensor at the beginning of each session. We defined each task based on the MDS-UPDRS part III as follows:

- **FT (MDS-UPDRS 3.4)**: Participants were instructed to tap their index finger on their thumb ten times as rapidly and as big as possible.
- **OC (MDS-UPDRS 3.5)**: Participants were instructed to open and close their hands ten times as fully and rapidly as possible. If the hand did not open or close sufficiently, participants were instructed how to perform the task correctly and then data collection was repeated.
- **PS (MDS-UPDRS 3.6)**: Participants were instructed to extend their arms forward with their palms facing down and alternately pronate and supinate their forearm by rotating the palm up and down alternately ten times as rapidly as possible.

Board-certified movement-disorder specialists (N.K., S.I.T., Y.T., and S.K.) examined these three tasks as performed using the left and right hands separately and rated them according to five characteristics: speed, amplitude, hesitations, halts, and decrementing amplitude (details are provided elsewhere [4]). This produced a data set encompassing 207 hand-gesture signals for FT, 207 for OC, and 206 for PS.

E. DATA ACQUISITION

The measurement setup is shown in Fig. 4. An acrylic stand served a dual purpose: (i) providing a comfortable platform for the participant to rest their hand during the examination and (ii) ensuring a consistent hand position relative to the LMD sensor, which was securely attached to a nonslip mat. Participants positioned their forearms on the inclined surface of the stand with their hand extended beyond the stand's edge and the palm facing the LMD sensor. The height of the stand was 15 cm. In addition, we placed a nonslip mat underneath the acrylic stand to anchor it in place and thereby prevent any unintended vibrations during the measurements.

F. DATA PREPROCESSING

As mentioned above, we utilized the LMD for collecting hand-gesture signals, which provided us with time-series

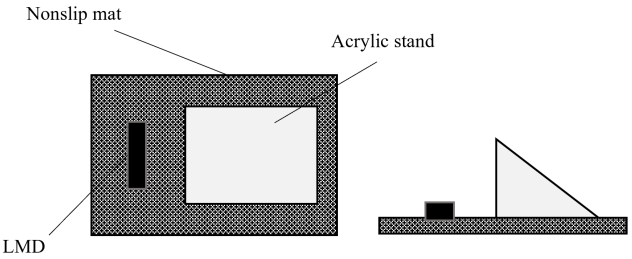

FIGURE 4. Measurement environment.

data, including on the finger joint positions and palm orientation. The LMD also provided information on various physical properties, such as bone lengths and hand visibility. However, we opted to exclude these physical properties from our analyses. Furthermore, to ensure uniformity in our data, we applied linear interpolation to standardize the sampling rate to 50 Hz, resulting in a constant data-point interval of 0.02 seconds.

G. MOVEMENT PATTERN ANALYSIS

Following data preprocessing, we computed two distinct movement patterns for each task as depicted in Fig. 5. For the FT task we computed two parameters: (i) FTdis represents the Euclidean distance between the index finger and thumb, and (ii) FTang denotes the angle formed between the index finger and thumb. For the OC task we computed OCdis, which represents the sum of the Euclidean distances between the palm center and the five fingertips. Additionally, OCang was derived from the angles formed by the middle and tip of each finger. For the PS task, we determined the palm angle based on the vector formed by the thumb to the little finger (PSang), along with the x-plane distance between the thumb and index finger (PSdis).

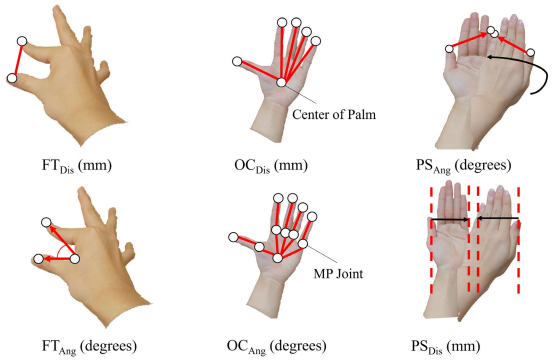

FIGURE 5. Movement patterns of MDS-UPDRS task.

We conducted a further extensive analysis by computing 15 different distances between 2 points from the palm and the five fingertips. We additionally calculated 14 distinct ranges of motion for each joint of the fingers. This resulted in the generation of 31 unique movement patterns for each task, encompassing movement-related parameters ($N = 2$), distances between 2 points ($N = 15$), and ranges of motion ($N = 14$).

TABLE 1. Names and descriptions of the extracted movement patterns.

Name of movement pattern	Description
Palm2{Thumb, Index, Middle, Ring, Little}	Distance from the palm position to the tip of the {thumb, index, middle, ring, little} finger.
Thumb2{Index, Middle, Ring, Little}	Distance from the tip of the thumb to the tip of the {index, middle, ring, little} finger.
Index2{Middle, Ring, Little}	Distance from the tip of the index finger to the tip of the {middle, ring, little} finger.
Middle2{Ring, Little}	Distance from the tip of the middle finger to the tip of the {ring, little} finger.
Ring2Little	Distance from the tip of the ring finger to the tip of the little finger.
Thumb_IP	Range of motion the interphalangeal joint
{Index,Middle,Ring,Little}_DIP	Range of motion the distal interphalangeal joint
{Index,Middle,Ring,Little}_PIP	Range of motion the proximal interphalangeal joint
{Thumb,Index,Middle,Ring,Little}_MP	Range of motion the metacarpophalangeal joint

It is worth noting that, in the case of the FT task, the movement pattern related to the task and the Thumb2Index parameter (i.e., distance from the tip of the thumb to the tip of the index finger) convey the same information. Therefore, the analysis of the FT task was based on 30 movement patterns (i.e., excluding Thumb2Index). A more-detailed description of these movement patterns and their respective names is provided in Table 1.

H. EXTREME-VALUE DETECTION

To focus the analysis on specific task segments, we manually extracted data based on distinct movement patterns, namely FTdis, OCdis, and PSang. It is important to note that while some data were obtained from more than 10 repetitions of a task, others had fewer repetitions; nevertheless, all available data were included in our analysis. From the extracted data we implemented the procedure described below for extreme-value detection.

1) FOURIER FILTER

The frequency of human hand movements is generally below 10 Hz. Therefore, to remove high-frequency noise with a cutoff frequency of 10 Hz. A lowpass cutoff of 10 Hz was also used in a previous study [33]. It should be noted that tremor in PD patients generally appears at 4–6 Hz [43]. Considering the Nyquist frequency, a lowpass filter with a cutoff of 10 Hz may influence the acquisition of information about the tremor components. However, this study focused on evaluating akinesia rather than tremor, and so we consider that lowpass filtering at 10 Hz is justifiable.

2) MOVING-AVERAGE FILTER

To further enhance data quality and address any gaps resulting from applying the Fourier transform, we employed a moving-average filter with a window size set at 2% of the data length.

I. EXTREME-VALUE DETECTION USING THE AMPD ALGORITHM

For the final stage of extreme value detection, we used the AMPD (automatic multiscale-based peak detection) algorithm to identify both local maxima and local minima [44]. However, it is important to note that there were instances where the algorithm did not accurately detect extreme values. In such cases, manual correction of the extreme values was performed. Fig. 6 presents the segmented data and graphs displaying detected extreme values for FTdis, OCdis, and PSang. Similar procedures were applied to other movement patterns at the same time.

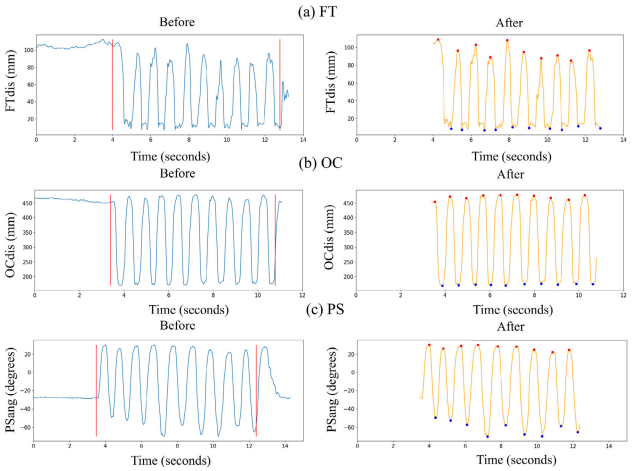

FIGURE 6. Hand gesture signals of PD patients before and after data processing during performing three tasks: (a) FT task; (b) OC task; and (c) PS task.

J. FEATURE EXTRACTION

To extract pertinent kinematic features, positive and negative peaks were initially identified by detecting local maxima and minima, respectively. We then computed various motion-quantification parameters such as velocity, frequency, amplitude, slope, and variance for each movement pattern. We additionally computed jitter and shimmer parameters in accordance with previous research [45], [46], [47]. Jitter quantifies the variation of the signal waveform along the time axis, while shimmer is associated with amplitude variations. Furthermore, we derived features using the tsfresh library [35] and the noise valiance [48], [49], which are independent of extreme values. Table 2 presents a comprehensive list of the extracted features obtained through this process.

K. FEATURE SELECTION

The performance of ML-based algorithms critically depends on the quality of input features. This study used an RF-based algorithm to order the input features based on the Gini impurity scores. At the same time, SFFS with an SVM was

TABLE 2. List of extracted features from raw features.

Features Names	Explanations	Computational Formula
Amplitude [37]	Mean envelope difference	$\frac{1}{N}\sum_{i=1}^{N}[X(\mathrm{PP}_i)-X(\mathrm{NP}_i)]$
Frequency (Freq) [37]	Inverse of the average peak-to-peak time	$\frac{1}{\frac{1}{N-1}\sum_{i=1}^{N-1}\mathrm{t}(PP_{i+1})-\mathrm{t}(PP_i)}$
Vel [37]	Average of absolute velocities	$\frac{1}{M-1}\sum_{i=1}^{M-1}\frac{\lvert X_{i+1}-X_i\rvert}{t_{i+1}-t_i}$
Slope [37]	Linear regression slope	[50]
Variance [37]	Variance after removing trends	
Total_Time [15]	Total time required to perform a task	$\mathrm{t}(NP_N)-\mathrm{t}(PP_1)$
Max_Max [15]	Maximum (Max) point among the Max points	Max(X(PP))
Max_Min [15]	Max point among the minimum (Min) points	Min(X (PP))
Min_Max [15]	Min point among the Max points	Max(X(NP))
Min_Min [15]	Min point among the Min points	Min(X(NP))
Avg_Max [15]	Average Max counting by Max points	$\frac{1}{N}\sum_{i=1}^{N}X(\mathrm{PP}_i)$
SD_Max [[15]	SD of Max points	$\sqrt{\frac{1}{N}\sum_{i=1}^{N}X(PP_i)-X(\bar{P}P)}$
Avg_Min [15]	Average Min counting by Min points	$\frac{1}{N}\sum_{i=1}^{N}X(\mathrm{NP}_i)$
SD_Min [15]	SD of minimum points	$\sqrt{\frac{1}{N}\sum_{i=1}^{N}X(NP_i)-X(\bar{N}P)}$
SD_Freq [15]	SD of frequency	$\sqrt{\frac{1}{N-1}\sum_{i=1}^{N-1}[Freq_i-\overline{Freq}]}$
Avg_Open_Speed [15]	Average opening speed	$\frac{1}{N-1}\sum_{i=1}^{N-1}\frac{\lvert X(\mathrm{PP}_{i+1})-X(\mathrm{NP}_i)\rvert}{t(\mathrm{PP}_{i+1})-t(\mathrm{NP}_i)}$
Avg_Clos_Speed [15]	Average closing speed opening	$\frac{1}{N}\sum_{i=1}^{N}\frac{\lvert X(\mathrm{PP}_i)-X(\mathrm{NP}_i)\rvert}{t(\mathrm{PP}_i)-t(\mathrm{NP}_i)}$
Max_Open_Speed [15]	Maximum opening speed	$Max(\frac{\lvert X(\mathrm{PP}_{i+1})-X(\mathrm{NP}_i)\rvert}{t(\mathrm{PP}_{i+1})-t(\mathrm{NP}_i)},\ i=1,2,..N-1)$
Min_Open_Speed [15]	Minimum opening speed	$Min(\frac{\lvert X(\mathrm{PP}_{i+1})-X(\mathrm{NP}_i)\rvert}{t(\mathrm{PP}_{i+1})-t(\mathrm{NP}_i)},\ i=1,2,..N-1)$
Max_Clos_Speed [15]	Maximum closing speed	$Max(\frac{\lvert X(\mathrm{PP}_i)-X(\mathrm{NP}_i)\rvert}{t(\mathrm{PP}_i)-t(\mathrm{NP}_i)},\ i=1,2,..N)$
Min_Clos_Speed [15]	Minimum closing speed	$Min(\frac{\lvert X(\mathrm{PP}_i)-X(\mathrm{NP}_i)\rvert}{t(\mathrm{PP}_i)-t(\mathrm{NP}_i)},\ i=1,2,..N)$
Avg_Open_Amp [15]	Average opening amplitude	$\frac{1}{N-1}\sum_{i=1}^{N-1}\lvert X(\mathrm{PP}_{i+1})-X(\mathrm{NP}_i)\rvert$
SD_Open_Amp [15]	SD of opening amplitude	$\sqrt{\frac{1}{N-1}\sum_{i=1}^{N-1}(OA_i-\overline{OA})^2}$
Max_Open_Amp [15]	Maximum opening amplitude	$Max(\lvert X(\mathrm{PP}_{i+1})-X(NP_i)\rvert,\ i=1,2,\ldots N-1)$
Min_open_amp [15]	Minimum opening amplitude	$Min(\lvert X(\mathrm{PP}_{i+1})-X(NP_i)\rvert,\ i=1,2,\ldots N-1)$
Avg_Clos_Amp [15]	Average closing amplitude	$\frac{1}{N}\sum_{i=1}^{N}\lvert X(\mathrm{PP}_i)-X(\mathrm{NP}_i)\rvert$
SD_Clos_Amp [15]	SD of closing amplitude (CA)	$\sqrt{\frac{1}{N}\sum_{i=1}^{N}(CA_i-\overline{CA})^2}$
Max_Clos_Amp [15]	Maximum closing amplitude	$Max(\lvert X(\mathrm{PP}_i)-X(\mathrm{NP}_i)\rvert, i=1,2,\ldots N)$
Min_Clos_Amp [15]	Minimum closing amplitude	$Min(\lvert X(\mathrm{PP}_i)-X(\mathrm{NP}_i)\rvert, i=1,2,\ldots N)$
N_Extrema	No. of extrema unrelated to task	$len\,(extrema\ in\ the\ graph)-len\,(PP)$
Tapping_Rate	Tapping frequency per second	$len\,(PP)/Total\ Time$
Amp_Delta [51]	Decrement ratio of amplitude	$(\mathrm{Amp}_{2nd\ half}-\mathrm{Amp}_{1st\ half})/\mathrm{Amp}_{1st\ half}$
CV_Amp [51]	CV of amplitude	$\sqrt{\frac{1}{N}\sum_{i=1}^{N}(\mathrm{Amp}_i-\bar{Amp})^2}/Amp$
Med_Period [33]	Median of period	$Med(t\,(PP_{i+1})-t\,(PP_i),\ i=1,2,..N-1)$
Med_Amp [33]	Median of amplitude	$Med(\frac{X(PP_{i+1})-X(PP_i)}{2}-X\,(NP_i),\ i=1,2,..N-1)$
Max_Period [33]	Max. value of period	$Max(t\,(PP_{i+1})-t\,(PP_i),\ i=1,2,..N-1)$
Period_Large_Num [33]	No. of elements the Med. period value	$len\,(t\,(PP_{i+1})-t\,(PP_i)>Med_{P}eriod);\ i=1,2,..N-1$
Min_Amp [33]	Min. value of amplitude	$Min(\frac{X(PP_{i+1})-X(PP_i)}{2}-X\,(NP_i),\ i=1,2,..N-1)$
Amp_Small_Num [33]	No. of elements smaller than the median value of amplitude	$len\left(\frac{X(PP_{i+1})-X(PP_i)}{2}-X\,(NP_i)>Min\_Amp\right);\ i=1,2,..N-1$
Shdb [45]	Mean absolute difference of the amplitude in decibels	$\frac{1}{N-1}\sum_{i=1}^{N-1}\lvert 20*\log\frac{\mathrm{Amp}_{i+1}}{\mathrm{Amp}_i}\rvert$
Shimmer_Rel [45]	Mean absolute value between consecutive amplitudes divided by the mean amplitude	$len\left(\frac{X(PP_{i+1})-X(PP_i)}{2}-X\,(NP_i)>Min\_Amp\right);\ i=1,2,..N-1$
Shimmer_Apq3 [45]	Quotient of the amplitude disturbance within three periods	$\frac{\frac{1}{N-2}\sum_{i=2}^{N-1}\lvert Amp(i)-\left(\frac{1}{3}\sum_{j=i-1}^{i+1}Amp(j)\right)\rvert}{\frac{1}{N}\sum_{i=1}^{N}Amp(i)}$
Jitter_Abs [45]	Mean absolute value between two consecutive periods	$\frac{1}{N-1}\sum_{i=1}^{N-1}\lvert Period(i+1)-Period(i)\rvert$
Jitter_Rel [45]	Mean absolute value between two consecutive periods divided by period average	$\frac{\frac{1}{N-1}\sum_{i=1}^{N-1}\lvert Period(i+1)-Period(i)\rvert}{\frac{1}{N}\sum_{i=1}^{N}Period(i)}$
Jitter_ppq3 [45]	Average disturbance	$\frac{\frac{1}{N-2}\sum_{i=2}^{N-1}\lvert Period(i)-\left(\frac{1}{3}\sum_{j=i-1}^{i+1}Period(j)\right)\rvert}{\frac{1}{N}\sum_{i=1}^{N}Period(i)}$
Noise_Var [48]	Noise variance	
Conv_Ene [49]	Amplitude sum of squares	$\sum_{i=1}^{M}{X_i}^2$
SNR [49]	Signal to noise ratios	$Conv_ene/Noise_var$
Amp_Var [35]	Variance of time-series amplitude d	$\frac{1}{M}\sum_{i=1}^{M}\left(X_i-\bar{X}\right)^2$
Amp_Avg_Abs_Change [35]	Average over first amplitude differences	$\frac{1}{M-1}\sum_{i=1}^{M-1}\lvert X_{i+1}-X_i\rvert$
Amp_Autocorr_Lagi [35]; i=1,...,9	Autocorrelation of the specified lag	[20]
Var_Vel [35]	Variance of time-series velocity	$\frac{1}{M}\sum_{i=1}^{M}(\mathrm{Vel}_i-\bar{Vel})^2$
Vel_Abs_Ener [35]	Absolute energy of the sum of squares of velocity	$\frac{1}{M-1}\sum_{i=1}^{M-1}\lvert \mathrm{Vel}_{i+1}-\mathrm{Vel}_i\rvert$
Vel_Quant_i ; i=0.1,0.2...0.4,0.6,0.7...0.9	Quantile of time-series velocity	[35]

Here, PPi: ith value of the positive peaks of a signal, which was determined by local maxima; NPi: ith value of the negative peaks of a signal, which was determined by local minima. N: Number of extrema; M: length of data. $\mathrm{Freq}_i=\frac{1}{t(\mathrm{PP}_{i+1})-t(\mathrm{PP}_i)}$; $\mathrm{Open\_Amp}_i=\lvert X\,(\mathrm{PP}_{i+1})-X\,(\mathrm{NP}_i)\rvert$;

$\mathrm{Clos\_Amp}_i=\lvert X\,(\mathrm{PP}_i)-X\,(\mathrm{NP}_i)\rvert$; $\mathrm{Amp}_i=X(PP_i)-X(NP_i)$; $Period_i=t(PP_{i+1})-t(PP_i)$; $\mathrm{Vel}_i=\frac{\lvert X_{i+1}-X_i\rvert}{t_{i+1}-t_i}$.

applied to three tasks to select the relevant combination of input features, which can be used for the prediction and classification of patients with PD. This study found that the OC tasks exhibited outstanding performance for identifying patients with PD.

In this study, we implemented two feature selection methods (RF and SFFS) to identify significant features for PD patients. We initially employed an RF-based algorithm to select the top 15% of features based on their Gini impurity scores. We then applied an SFFS-based algorithm to the top

TABLE 3. Range of parameter tuning for RF.

Parameters	Description	Range
n_estimators	Number of trees	1~200 (int)
criterion	Function to measure the quality of a split	['gini','entropy','log_loss']
max_depth	Maximum depth of the tree	1~1000 (int)
min_samples_split	Minimum no. of samples required to split an internal node	2~5 (int)
min_samples_leaf	Minimum no. of samples required to be at a leaf node	1~10 (int)
max_features	Number of features to consider when looking for the best split	[None,'sqrt','log2']
max_leaf_nodes	Maximum number of leaves in the tree	2~1000 (int)
bootstrap	Whether bootstrap samples are used when building trees	[True,False]

15% features, which were initially selected by the RF-based algorithm. Concise explanations of these two algorithms are provided below.

1) RANDOM FOREST

RF is a supervised method that combines two techniques: (i) decision tree and (ii) ensemble learning [52]. It is widely used for classification and feature selection. In our study we employed an RF-based model to identify top-ranking features using the following steps:

- N sets of subsamples were created from the original data using the bootstrap method through random sampling.
- N decision trees were generated, each using one of the subsamples.
- Nodes were created according to the following method until the specified number of nodes was reached: randomly selecting M explanatory variables and then constructing a decision tree.
- The RF model was trained using LOOCV and its hyperparameters were optimized. The range of the hyperparameters for the RF-based model, as presented in Table 3, were optimized using Optuna.
- The RF-based model was then retrained and the Gini impurity was computed.
- The Gini impurity values were sorted into descending order.
- Finally, the top 15% of features were selected based on their Gini impurity scores.

2) SFFS-BASED ALGORITHM

SFFS is widely used to select a subset of k-dimensional features from a d-dimensional feature space (where $k<d$), and plays a crucial role in enhancing generalization errors [53]. In the present study, we employed SFFS to select relevant features for PD patients across the FT, OC, and PS tasks after identifying an initial 15% of potential features to expedite computations. The detailed steps of the SFFS-based algorithm are comprehensively documented elsewhere [27], [28], [53].

L. CLASSIFICATION USING AN SVM

An SVM is one of the most robust supervised learning models, and was initially proposed by Cortes and Vapnik in 1995 [54]. SVMs excel in classifying both linear and nonlinear data through kernel methods, by optimizing the margin of the hyperplane. In this study we employed an SVM to identify a hyperplane that effectively classifies PD patients into five categories (normal, slight, mild, moderate, and severe), addressing the following problems:

$$\max \alpha \sum_{i=1}^{n} \alpha_i - \frac{1}{2} \sum_{i=1}^{n} \sum_{j=1}^{n} \alpha_i \alpha_j y_i y_j K(x_i, x_j) \tag{1}$$

subject to

$$\sum_{i=1}^{n} {y_i}^T \alpha_i = 1,\ 0 \le \alpha_i \le C, i = 1, \ldots, n\ \forall\, i = 1,\ 2, , 3, \ldots, n \tag{2}$$

The final discriminate function takes the following form:

$$f(x) = \sum_{i=1}^{n} \alpha_i K(x_i, x_j) + b \tag{3}$$

where b is the bias term.

This study employed an SVM with RBF and sigmoid kernels for classifying PD patients. The computation formulae for these kernels are as follows:

$$RBF : K(x_i, x_j) = \exp(-\gamma \|x_i - x_j\|^2);\ \gamma > 0 \tag{4}$$

$$\text{Sigmoid Kernel} : K(x_i, x_j) = \tanh(k x_i . x_j + c) \tag{5}$$

IV. EXPERIMENTAL SETUP AND PERFORMANCE METRICS

A. EXPERIMENTAL SETUP

All experiments were performed on a Windows 11 computer. Data were obtained using an LMD with two distinct API versions: versions 3.2 and version 4.1.0. The data were analyzed using Python (version 3.10.9). For classification, we adopted the SVM algorithm with LOOCV and fine-tuned hyperparameters using Optuna. To optimize the SVM parameters effectively, we defined the parameter ranges as follows: kernel: 'rbf', 'sigmoid', cost: (ranging from 0.01 to 100), and γ: (ranging from 0.01 to 100). The optimization process comprised 200 trials, and the seed value was fixed at 42.

B. PERFORMANCE METRICS

We trained an SVM model for predicting patients with PD, and simultaneously constructed a confusion matrix by comparing predicted classes against actual classes. We employed four performance metrics (accuracy, recall, precision, and F1 score) to assess the performance of the SVM model. These performance metrics can be easily computed from the confusion matrix; their formulae have already been clearly explained elsewhere [21], [22].

TABLE 4. Baseline characteristics of patients with PD for right-handed with FT task.

Variables	Overall	Normal	Slight	Mild	Moderate	Severe	p-value[1]
Overall, n (%)	45	12 (26.7)	13 (28.9)	12 (26.7)	7 (15.6)	1 (2.2)	
Age, Mean±SD	69.8±10.1	69.2± 10.5	66.3±8.9	70.8 ± 12.6	74.7 ± 5.3	76.0 ± 0.0	0.453
Gender							
Male, n (%)	28 (62.2)	6 (35.3)	4 (23.5)	4 (23.5)	2 (11.8)	1 (5.9)	0.552
Female, n (%)	17(37.8)	6 (21.4)	9 (32.1)	8 (28.6)	5 (17.9)	0 (0.00)	

Note: p-value is obtained from one-way ANOVA test and a chi-square test for age and sex variables, respectively.

V. EXPERIMENTAL RESULTS AND DISCUSSION

A. BASELINE CHARACTERISTICS OF PATIENTS WITH PD PATIENTS

This study enrolled a cohort of 45 PD patients aged 69.8±10.1 years (mean±SD) and including 62.2% males. Table 4 provides an overview of the baseline characteristics of PD patients performing the FT task with their right hand. There was no significant difference in age or sex among patients with normal, slight, mild, moderate, and severe PD symptoms.

B. CLASS DISTRIBUTION OF PD PATIENTS

We collected hand-gesture signals from the PD patients and classified them into five categories (slight, mild, moderate, and severe) based on their respective MDS-UPDRS scores for both the left and right hands when performing each of the three tasks (FT, OC, and PS). The distribution of PD patients across these categories is presented in Table 5.

TABLE 5. Class distribution of patients with PD when performing the FT, OC, and PS tasks with the left and right hands.

Class	FT	OC	PS
Normal	60	76	49
Slight	65	61	54
Mild	45	57	56
Moderate	33	12	46
Severe	4	1	1
Total	207	207	206

C. RESULTS FROM FEATURE EXTRACTION

We computed 31 distinct movement patterns for each task. Of these patterns, 2 movement patterns were related to the task, 15 were related to distances between 2 points, and the remaining 14 were related to the ranges of motion. These movement patterns were used to derive 69 statistical features. The computational formulae for these statistical features are provided in Table 2 for clarity. This comprehensive process yielded 2139 features (69 features per pattern multiplied by 31 patterns), which were utilized in both the RF-based algorithm and the SFFS-based feature-selection model to identify the most-relevant features for diagnosing patients with PD.

D. RESULTS FROM THE FEATURE-SELECTION AND CLASSIFICATION MODELS

After extracting 2139 features, we applied the RF-based algorithm to compute the Gini impurity scores for each feature. We then ranked the features in descending order of Gini impurity scores and selected the top 15% of features; that is, 321 of the original 2139. These 321 features were fed into the SFFS process with an SVM model to classify patients with PD. In this study we used LOOCV to train SFFS with the SVM model and fine-tuned the hyperparameters of SVM using Optuna.

These tuning efforts were performed separately for the FT, OC, and PC tasks. During the training phase, we systematically explored two kernel functions (RBF and sigmoid) and set the cost and γ to various values within the range from 0.01 to 100. Our approach involved conducting 200 trials with the seed value fixed at 42. Upon optimizing the parameters, we retrained SFFS with an SVM model for (N-1) patients with PD, reserving one patient as a test set for predictive evaluations. This procedure was repeated in N iterations. Our observations revealed that SFFS with an SVM algorithm yielded the highest performance scores for the FT, OC, and PS tasks, each employing distinct combinations of 12, 14, and 12 features, respectively. Furthermore, we constructed confusion matrices (Fig. 7) by contrasting the actual class against the predicted class labels for the FT, OC, and PS tasks.

TABLE 6. Classification performance (in %) of the SVM for predicting the presence of PD in patients performing the FT, OC, and PS tasks.

Tasks	Accuracy	Precision	Recall	F1-score
FT	87.0	89.5	83.3	85.9
OC	93.2	76.1	73.2	74.4
PS	92.2	74.0	74.0	73.9

We computed various performance metrics from these confusion matrices (including the classification accuracy, recall, precision, and F1 -score) for the FT, OC, and PS tasks, as presented in Table 6. Notably, the SVM demonstrated remarkable performance with a classification accuracy of 87.0% for FT, 93.2% for OC, and 92.2% for PS. It is worth highlighting that the classification accuracy of the SVM was achieved the highest for the OC task. Furthermore, we observed that the SVM exhibited a recall rate of 73.2%, precision of 76.1%, and F1-score of 74.4% for the OC task. From these results, we concluded that the OC task is a promising tool for detecting patients with PD.

The ROC curves of the SVM for the multiclass prediction of patients with PD across the FT, OC, and PS tasks are presented in Fig. 8. ROC curves represent the change in false-positive and true-positive rates when the threshold is changed. Each graph in Fig. 8 shows ROC curves for the micro average, the macro average, and the normal, slight,

TABLE 7. AUC values for the FT, OC, and PS tasks.

Tasks	Micro-Avg.	Macro-Avg.	Normal	Slight	Mild	Moderate	Severe
FT	0.92	0.90	0.95	0.92	0.88	0.87	0.88
OC	0.96	0.86	0.95	0.96	0.96	0.92	0.50
PS	0.95	0.86	0.94	0.94	0.97	0.94	0.50

TABLE 8. Statistical validation of selected features from SFFS for the FT, OC, and PS tasks.

FT		OC		PS	
Feature	p-value[1]	Features	p-value[1]	Features	p-value[1]
Thumb2Little_Vel_Quant_0.9	<0.001	Little_PIP_Min_Clos_Speed	<0.001	PSdis_Vel_Quant_0.3	<0.001
Little_DIP_Min_Min	0.017	Ring_PIP_Conv_Ene	<0.001	PSang_Avg_Min	<0.001
Palm2Little_Var_Vel	0.062	Little_DIP_Avg_Min	0.012	Index2Ring_Vel_Quant_0.4	<0.001
FTang_Amp_Var	<0.001	Thumb2Ring_Amp_Autocorr_Lag6	0.021	PSdis_Avg_Open_Amp	0.011
Middle_MP_Min_Min	0.033	Thumb2Little_Avg_Max	<0.001	Index2Middle_Max_Min	<0.001
Index_MP_Amplitude	0.061	Thumb2Index_Min_Min	0.037	Palm2Middle_Avg_Max	0.006
Middle2Ring_Vel_Quant_0.4	0.475	Little_PIP_Avg_Open_Speed	<0.001	Little_PIP_Avg_Max	0.0008
Palm2Index_Max_Max	0.092	Ring_PIP_Amplitude	<0.001	Index2Little_Conv_Ene	0.005
Index2Ring_Conv_Ene	0.001	Thumb2Index_Max_Max	0.0008	Index_DIP_Med_Peirod	<0.001
Thumb2Little_Vel_Quant_0.1	<0.001	Palm2Thumb_Min_Max	<0.001	PSang_Amplitude	<0.001
FTdis_Amp_Avg_Abs_Change	<0.001	Thumb_MP_Conv_Ene	<0.001	Thumb2Middle_Avg_Min	0.014
Palm2Little_Amp_Var	0.199	Index_PIP_Max_Max	0.019	PSang_Vel_Abs_Ene	<0.001
		Middle2Ring_Max_Min	0.965		
		Ring_DIP_Avg_Max	0.006		

[1] p-value is obtained from one-way ANOVA.

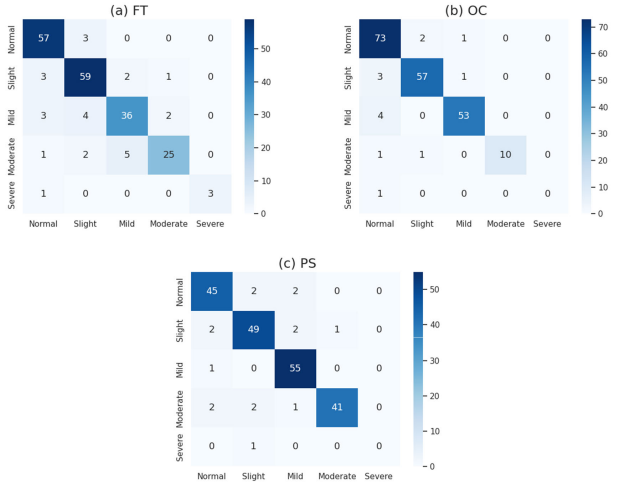

FIGURE 7. Confusion matrix for three tasks: (a) FT; (b) OC; and (c) PS.

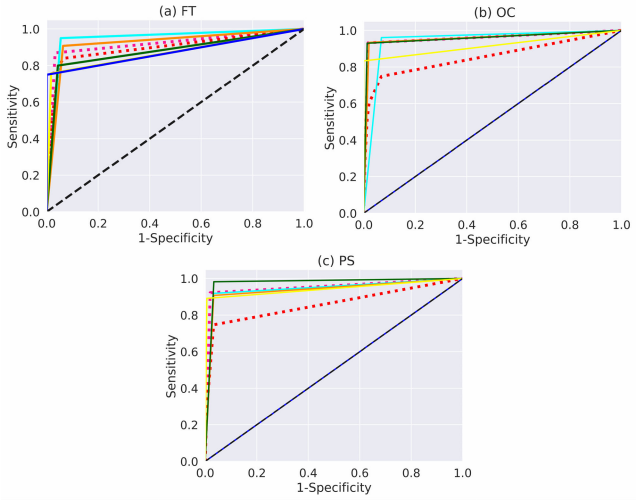

FIGURE 8. ROC curve for multiclass over three tasks: (a) FT, (b) OC, and (c) PS. The curves that each color represents are as follows: Magenta: Micro-average, Red:Macro-average, Cyan:Normal, Orange:Slight, Green:Mild, Yellow:Moderate, Blue:Severe.

mild, moderate, and severe categories. The micro-average indicates the overall performance by considering each class as a single class, while the macro average is the average of the curves for each class and their respective AUC scores in each task, as presented in Table 7. The SVM attained the highest micro-average AUC value of 0.96 for the OC task. This indicates that the OC task is the most-effective and discerning task for detecting patients with PD.

E. STATISTICAL VALIDATION OF SELECTED FEATURES

We applied one-way analysis of variance (ANOVA) to the results described in the previous section. We also computed the p-value for each feature in the context of all three tasks. The results are presented in Table 8. It is evident from Table 8 that 7 features for FT, 13 features for OC, and 12 features for PS exhibited statistical significance in relation to patients with PD. We conclude that using the LMD with the OC task is a promising method for detecting patients with PD.

F. COMPARISON WITH A PREVIOUS STUDY

This section describes a comparative analysis between the performance of our proposed system and that of a previous study, as presented in Table 9. Chen et al. [33] proposed the PD-Net system for detecting PD patients based on hand gestures. Their approach consisted of three steps: (i) detecting 21 key locations on the hand from RGB videos, (ii) analyzing movement patterns to identify the temporal patterns of these key locations on the hand and the motor symptoms, and (iii) predicting MDS-UPDRS scores based on the identified features. Their results indicated a classification accuracy of

TABLE 9. Comparison between this study against a previous study.

Authors	Device	Task	Target & Class	Classifier	Accuracy (%)
Chen et al. [33]	Video	FT, OC, PS	UPDRS score & 5 class	RF	FT: 85.7 OC: 89.3 PS: 88.6
This study	Leap Motion	FT, OC, PS	UPDRS score & 5 class	SVM	FT: 87.0 OC: 93.2 PS: 92.2

85.7% for FT, 89.3% for OC, and 88.7% for PS. In our study we also proposed an ML-based patient-detection system. We extracted features not only from the actual motor task but also from the movements of other joints. The identified features were ranked using an RF-based model based on their descending order of Gini impurity scores. The top 15% of features were then used in SFFS with an SVM model to identify the most-relevant combination of features. Our approach achieved a classification accuracy of 87.0% for FT, 93.2% for OC, and 92.2% for PS, which represents a notably better performance than that achieved in the study of Chen et al. [33].

VI. CONCLUSION, LIMITATIONS, AND FUTURE WORK

This study proposed an ML-based PD detection system based on the analysis of hand gestures. Our proposed system comprised several steps: (i) collecting hand-gesture signals using LMD sensors while performing FT, OC, and PS tasks; (ii) identifying movement patterns and then extracting statistical features from each movement pattern; (iii) applying an RF-based algorithm to rank features based on the classification accuracy, and then selecting the top 15% of features; (iv) implementing SFFS with an SVM model to determine relevant feature combinations based on the Gini impurity scores; and (v) applying one-way ANOVA to assess the statistical significance of selected features and evaluating their discriminative power. This study has demonstrated that our proposed system achieved impressive results, with an accuracy of 87.0% for FT, 93.2% for OC, and 92.2% for PS. Additionally, our findings highlighted the efficacy of using 12 specific features of OC tasks to classify patients with PD. We anticipate that this proposed system will prove invaluable to physicians in assessing motor symptoms in PD patients.

Despite achieving outstanding performance, this study had several limitations. First, there was an imbalance in the distribution of the data according to severity grading, with only a small amount of data on the most-severe cases. Future studies should confirm the present results by analyzing a more-balanced dataset. We used an SVM in our study due to the small amount of data. However, DL models should also be developed to achieve more accurate diagnosis. Second, we only evaluated akinesia. Future studies using sensor devices should develop a more-comprehensive approach that incorporates all of the cardinal Parkinsonian features; that is, akinesia, rigidity, and tremor. Third, we focused only on hand symptoms, whereas PD symptoms appear throughout the body. Sensor-based methods for evaluating posture, leg movements, and gait should therefore be developed. Fourth, this study targeted PD patients, but there are other disorders that manifest parkinsonism, such as progressive supranuclear palsy and multiple-system atrophy. More evidence is needed on how the present tool works on the disorders with atypical parkinsonism and also whether it can discriminate among these disorders.

A. INSTITUTIONAL REVIEW BOARD STATEMENT

This study involved human subjects, and all ethical and experimental procedures were conducted in accordance with the principles outlined in the Declaration of Helsinki. Ethical approval and protocol clearance were obtained from the ethics review committees of both medical universities where participants were recruited and examined, as well as from the University of Aizu, where data analysis was conducted. All procedures were executed with unwavering commitment to ethical standards and guidelines.

ACKNOWLEDGMENT

This study was supported by the Japan Society for the Promotion of Science (JSPS) Grants-in-Aid for Scientific Research (KAKENHI), Japan, under Grant JP20H04493.

REFERENCES

[1] W. Poewe, K. Seppi, C. M. Tanner, G. M. Halliday, P. Brundin, J. Volkmann, A.-E. Schrag, and A. E. Lang, "Parkinson disease," *Nature Rev. Disease primers*, vol. 3, no. 1, pp. 1–21, 2017.

[2] J. Jankovic, "Parkinson's disease: Clinical features and diagnosis," *J. Neurol. Neurosurgery Psychiatry*, vol. 79, no. 4, pp. 368–376, 2008.

[3] R. B. Postuma, D. Berg, M. Stern, W. Poewe, C. W. Olanow, W. Oertel, J. Obeso, K. Marek, I. Litvan, A. E. Lang, G. Halliday, C. G. Goetz, T. Gasser, B. Dubois, P. Chan, B. R. Bloem, C. H. Adler, and G. Deuschl, "MDS clinical diagnostic criteria for Parkinson's disease," *Movement Disorders*, vol. 30, no. 12, pp. 1591–1601, Oct. 2015.

[4] J. S. Perlmutter, "Assessment of Parkinson disease manifestations," *Current Protocols Neurosci.*, vol. 49, no. 1, pp. 1–10, Oct. 2009.

[5] C. G. Goetz et al., "Movement disorder society-sponsored revision of the unified Parkinson's disease rating scale (MDS-UPDRS): Scale presentation and clinimetric testing results," *Movement Disorders, J. Movement Disorder Soc.*, vol. 23, no. 15, pp. 2129–2170, 2008.

[6] C. G. Goetz and G. T. Stebbins, "Assuring interrater reliability for the UPDRS motor section: Utility of the UPDRS teaching tape," *Movement Disorders*, vol. 19, no. 12, pp. 1453–1456, Dec. 2004.

[7] R. Deb, G. Bhat, S. An, H. Shill, and U. Y. Ogras, "Trends in technology usage for Parkinson's disease assessment: A systematic review," *MedRxiv*, Feb. 2021, doi: 10.1101/2021.02.01.21250939.

[8] E. Tolosa, G. Wenning, and W. Poewe, "The diagnosis of Parkinson's disease," *Lancet Neurol.*, vol. 5, no. 1, pp. 75–86, 2006.

[9] Y. Su, C. R. Allen, D. Geng, D. Burn, U. Brechany, G. D. Bell, and R. Rowland, "3-D motion system ('data-gloves'): Application for Parkinson's disease," *IEEE Trans. Instrum. Meas.*, vol. 52, no. 3, pp. 662–674, Jun. 2003.

[10] J. H. Choi, H.-I. Ma, Y. J. Kim, and U. Lee, "Development of an assessment method of forearm pronation/supination motor function based on mobile phone accelerometer data for an early diagnosis of Parkinson's disease," *Int. J. Bio-Science Bio-Technol.*, vol. 8, no. 2, pp. 1–10, Apr. 2016.

[11] A. Salarian, H. Russmann, C. Wider, P. R. Burkhard, F. J. G. Vingerhoets, and K. Aminian, "Quantification of tremor and bradykinesia in Parkinson's disease using a novel ambulatory monitoring system," *IEEE Trans. Biomed. Eng.*, vol. 54, no. 2, pp. 313–322, Feb. 2007.

[12] Z. Zhang, R. Hong, A. Lin, X. Su, Y. Jin, Y. Gao, K. Peng, Y. Li, T. Zhang, H. Zhi, Q. Guan, and L. Jin, "Automated and accurate assessment for postural abnormalities in patients with Parkinson's disease based on Kinect and machine learning," *J. NeuroEngineering Rehabil.*, vol. 18, no. 1, pp. 1–10, Dec. 2021.

[13] B. Dror, E. Yanai, A. Frid, N. Peleg, N. Goldenthal, I. Schlesinger, H. Hel-Or, and S. Raz, "Automatic assessment of Parkinson's disease from natural hands movements using 3D depth sensor," in *Proc. IEEE 28th Conv. Electr. Electron. Engineers Isr. (IEEEI)*, Dec. 2014, pp. 1–5.

[14] B. Galna, G. Barry, D. Jackson, D. Mhiripiri, P. Olivier, and L. Rochester, "Accuracy of the Microsoft Kinect sensor for measuring movement in people with Parkinson's disease," *Gait Posture*, vol. 39, no. 4, pp. 1062–1068, Apr. 2014.

[15] A. Moshkova, A. Samorodov, N. Voinova, A. Volkov, E. Ivanova, and E. Fedotova, "Parkinson's disease detection by using machine learning algorithms and hand movement signal from LeapMotion sensor," in *Proc. 26th Conf. Open Innov. Assoc. (FRUCT)*, Apr. 2020, pp. 321–327.

[16] E. Gamboa, A. Serrato, J. Castro, D. Toro, and M. Trujillo, "Advantages and limitations of leap motion from a Developers', physical Therapists', and Patients' perspective," *Methods Inf. Med.*, vol. 59, no. 2, pp. 110–116, May 2020.

[17] A. Z. B. Aziz, M. A. M. Hasan, S. Ahmad, M. A. Mamun, J. Shin, and M. R. Hossain, "IACP-MultiCNN: Multi-channel CNN based anticancer peptides identification," *Anal. Biochemistry*, vol. 650, Aug. 2022, Art. no. 114707.

[18] M. A. M. Hasan, M. Maniruzzaman, and J. Shin, "Identification of key candidate genes for IgA nephropathy using machine learning and statistics based bioinformatics models," *Sci. Rep.*, vol. 12, no. 1, p. 13963, Aug. 2022.

[19] J. Shin, S. Konnai, M. Maniruzzaman, M. A. M. Hasan, K. Hirooka, A. Megumi, and A. Yasumura, "Identifying ADHD for children with coexisting ASD from fNIRs signals using deep learning approach," *IEEE Access*, vol. 11, pp. 82794–82801, 2023.

[20] M. A. M. Hasan, M. Maniruzzaman, and J. Shin, "Differentially expressed discriminative genes and significant meta-hub genes based key genes identification for hepatocellular carcinoma using statistical machine learning," *Sci. Rep.*, vol. 13, no. 1, p. 3771, Mar. 2023.

[21] M. Maniruzzaman, M. A. M. Hasan, N. Asai, and J. Shin, "Optimal channels and features selection based ADHD detection from EEG signal using statistical and machine learning techniques," *IEEE Access*, vol. 11, pp. 33570–33583, 2023.

[22] M. Maniruzzaman, J. Shin, M. A. M. Hasan, and A. Yasumura, "Efficient feature selection and machine learning based ADHD detection using EEG signal," *Comput., Mater. Continua*, vol. 72, no. 3, pp. 5179–5195, 2022.

[23] S. Uddin, A. Khan, M. E. Hossain, and M. A. Moni, "Comparing different supervised machine learning algorithms for disease prediction," *BMC Med. Informat. Decis. Making*, vol. 19, no. 1, pp. 1–16, Dec. 2019.

[24] C. Ricciardi, M. Amboni, C. De Santis, G. Ricciardelli, G. Improta, L. Iuppariello, G. D'Addio, P. Barone, and M. Cesarelli, "Classifying different stages of Parkinson's disease through random forests," in *Proc. 15th Medit. Conf. Med. Biol. Eng. Comput. (MEDICON)*, Coimbra, Portugal. Cham, Switzerland: Springer, Sep. 2019, pp. 1155–1162, doi: 10.1007/978-3-030-31635-8_140.

[25] J. M. Templeton, C. Poellabauer, and S. Schneider, "Classification of Parkinson's disease and its stages using machine learning," *Sci. Rep.*, vol. 12, no. 1, p. 14036, 2022.

[26] J. Wiens and E. S. Shenoy, "Machine learning for healthcare: On the verge of a major shift in healthcare epidemiology," *Clin. Infectious Diseases*, vol. 66, no. 1, pp. 149–153, Jan. 2018.

[27] M. A. M. Hasan, J. Shin, and M. Maniruzzaman, "Online kanji characters based writer identification using sequential forward floating selection and support vector machine," *Appl. Sci.*, vol. 12, no. 20, p. 10249, Oct. 2022.

[28] J. Shin, M. Maniruzzaman, Y. Uchida, M. A. M. Hasan, A. Megumi, and A. Yasumura, "Handwriting-based ADHD detection for children having ASD using machine learning approaches," *IEEE Access*, vol. 11, pp. 84974–84984, 2023.

[29] J. C. Vásquez-Correa, T. Arias-Vergara, J. R. Orozco-Arroyave, B. Eskofier, J. Klucken, and E. Nöth, "Multimodal assessment of Parkinson's disease: A deep learning approach," *IEEE J. Biomed. Health Informat.*, vol. 23, no. 4, pp. 1618–1630, Jul. 2019.

[30] J. D. Loaiza Duque, A. M. González-Vargas, A. J. Sánchez Egea, and H. A. González Rojas, "Using machine learning and accelerometry data for differential diagnosis of Parkinson's disease and essential tremor," in *Proc. Workshop Eng. Appl.* Cham, Switzerland: Springer, 2019, pp. 368–378, doi: 10.1007/978-3-030-31019-6_32.

[31] P. M. Aubin, A. Serackis, and J. Griskevicius, "Support vector machine classification of Parkinson's disease, essential tremor and healthy control subjects based on upper extremity motion," in *Proc. Int. Conf. Biomed. Eng. Biotechnol.*, May 2012, pp. 900–904.

[32] D. Surangsrirat, C. Thanawattano, R. Pongthornseri, S. Dumnin, C. Anan, and R. Bhidayasiri, "Support vector machine classification of Parkinson's disease and essential tremor subjects based on temporal fluctuation," in *Proc. 38th Annu. Int. Conf. IEEE Eng. Med. Biol. Soc. (EMBC)*, Aug. 2016, pp. 6389–6392.

[33] Y. Chen, H. Ma, J. Wang, J. Wu, X. Wu, and X. Xie, "PD-Net: Quantitative motor function evaluation for Parkinson's disease via automated hand gesture analysis," in *Proc. 27th ACM SIGKDD Conf. Knowl. Discovery Data Mining*, Aug. 2021, pp. 2683–2691.

[34] Z. Guo, W. Zeng, T. Yu, Y. Xu, Y. Xiao, X. Cao, and Z. Cao, "Vision-based finger tapping test in patients with Parkinson's disease via spatial–temporal 3D hand pose estimation," *IEEE J. Biomed. Health Informat.*, vol. 26, no. 8, pp. 3848–3859, Aug. 2022.

[35] M. Christ, N. Braun, J. Neuffer, and A. W. Kempa-Liehr, "Time series FeatuRe extraction on basis of scalable hypothesis tests (tsfresh—A Python package)," *Neurocomputing*, vol. 307, pp. 72–77, Sep. 2018.

[36] A. Dadashzadeh, A. Whone, M. Rolinski, and M. Mirmehdi, "Exploring motion boundaries in an end-to-end network for vision-based Parkinson's severity assessment," 2020, *arXiv:2012.09890*.

[37] A. H. Butt, E. Rovini, C. Dolciotti, G. De Petris, P. Bongioanni, M. C. Carboncini, and F. Cavallo, "Objective and automatic classification of Parkinson disease with leap motion controller," *Biomed. Eng. OnLine*, vol. 17, no. 1, pp. 1–21, Dec. 2018.

[38] F. Weichert, D. Bachmann, B. Rudak, and D. Fisseler, "Analysis of the accuracy and robustness of the leap motion controller," *Sensors*, vol. 13, no. 5, pp. 6380–6393, May 2013.

[39] J. Guna, G. Jakus, M. Pogačnik, S. Tomažič, and J. Sodnik, "An analysis of the precision and reliability of the leap motion sensor and its suitability for static and dynamic tracking," *Sensors*, vol. 14, no. 2, pp. 3702–3720, Feb. 2014.

[40] *'Ultraleap' Leap Motion Coordinate Systems*. Accessed: Dec. 22, 2022. [Online]. Available: https://developer-archive.leapmotion.com/documentation/objc/devguide/Leap_Coordinate_Mapping.html

[41] A. Vysocký, S. Grushko, P. Oščádal, T. Kot, J. Babjak, R. Jánoš, M. Sukop, and Z. Bobovský, "Analysis of precision and stability of hand tracking with leap motion sensor," *Sensors*, vol. 20, no. 15, p. 4088, Jul. 2020.

[42] *Ultraleap, Leap Motion C API*. Accessed: Sep. 15, 2022. [Online]. Available: https://developer.leapmotion.com/documentation/v4/concepts.html

[43] P. Y. Chan, Z. M. Ripin, S. A. Halim, W. N. Arifin, A. S. Yahya, G. B. Eow, K. Tan, J. Y. Hor, and C. K. Wong, "Motion characteristics of subclinical tremors in Parkinson's disease and normal subjects," *Sci. Rep.*, vol. 12, no. 1, p. 4021, 2022.

[44] F. Scholkmann, J. Boss, and M. Wolf, "An efficient algorithm for automatic peak detection in noisy periodic and quasi-periodic signals," *Algorithms*, vol. 5, no. 4, pp. 588–603, Nov. 2012.

[45] M. A. Motin, N. D. Pah, S. Raghav, and D. K. Kumar, "Parkinson's disease detection using smartphone recorded phonemes in real world conditions," *IEEE Access*, vol. 10, pp. 97600–97609, 2022.

[46] A. Anjos de Oliveira, M. Dajer, P. Fernandes, and J. Teixeira, "Clustering of voice pathologies based on sustained voice parameters," in *Proc. 13th Int. Joint Conf. Biomed. Eng. Syst. Technol.*, 2020, pp. 280–287.

[47] J. P. Teixeira, J. F. T. Fernandes, F. L. Teixeira, and P. O. Fernandes, "Acoustic analysis of chronic laryngitis-statistical analysis of sustained speech parameters," in *Proc. 11th Int. Joint Conf. Biomed. Eng. Syst. Technol.*, 2018, pp. 168–175.

[48] D. Garcia, "Robust smoothing of gridded data in one and higher dimensions with missing values," *Comput. Statist. Data Anal.*, vol. 54, no. 4, pp. 1167–1178, Apr. 2010.

[49] P. Drotár, J. Mekyska, I. Rektorová, L. Masarová, Z. Smékal, and M. Faundez-Zanuy, "Decision support framework for Parkinson's disease based on novel handwriting markers," *IEEE Trans. Neural Syst. Rehabil. Eng.*, vol. 23, no. 3, pp. 508–516, May 2015.
[50] L. Marsili, G. Rizzo, and C. Colosimo, "Diagnostic criteria for Parkinson's disease: From James Parkinson to the concept of prodromal disease," *Frontiers Neurol.*, vol. 9, p. 156, Mar. 2018.
[51] J. Wu, N. Yu, Y. Yu, H. Li, F. Wu, Y. Yang, J. Lin, J. Han, and S. Liang, "Intraoperative quantitative measurements for bradykinesia evaluation during deep brain stimulation surgery using leap motion controller: A pilot study," *Parkinson's Disease*, vol. 2021, pp. 1–7, Jun. 2021.
[52] L. Breiman, "Random forests," *Mach. Learn.*, vol. 45, pp. 5–32, Oct. 2001.
[53] P. Pudil, J. Novovičová, and J. Kittler, "Floating search methods in feature selection," *Pattern Recognit. Lett.*, vol. 15, no. 11, pp. 1119–1125, Nov. 1994.
[54] C. Cortes and V. Vapnik, "Support-vector networks," *Mach. Learn.*, vol. 20, pp. 273–297, Sep. 1995.

JUNGPIL SHIN (Senior Member, IEEE) received the B.Sc. degree in computer science and statistics and the M.Sc. degree in computer science from Pusan National University, South Korea, in 1990 and 1994, respectively, and the Ph.D. degree in computer science and communication engineering from Kyushu University, Japan, in 1999, under a scholarship from the Japanese Government (MEXT). He was an Associate Professor, a Senior Associate Professor, and a Full Professor with the School of Computer Science and Engineering, The University of Aizu, Japan, in 1999, 2004, and 2019, respectively. He has coauthored more than 350 published papers for widely cited journals and conferences. His research interests include pattern recognition, image processing, computer vision, machine learning, human–computer interaction, non-touch interfaces, human gesture recognition, automatic control, Parkinson's disease diagnosis, ADHD diagnosis, user authentication, machine intelligence, handwriting analysis, recognition, and synthesis. He is a member of ACM, IEICE, IPSJ, KISS, and KIPS. He served as the program chair and a program committee member for numerous international conferences. He serves as a reviewer for several major IEEE and SCI journals. He serves as an Editor for IEEE journals, Springer, Sage, Taylor & Francis, *Sensors* (MDPI), *Electronics* (MDPI), and Tech Science.

MASAHIRO MATSUMOTO received the bachelor's degree in computer science and engineering from The University of Aizu (UoA), Japan, in March 2023, where he is currently pursuing the master's degree. He joined the Pattern Processing Laboratory, UoA, in April 2022, under the supervision of Dr. Jungpil Shin. His research interests include computer vision, pattern recognition, and deep learning. He is currently working on human activity recognition, human gesture recognition, and Parkinson's disease diagnosis.

MD. MANIRUZZAMAN received the B.Sc., M.Sc., and M.Phil. degrees in statistics from the Department of Statistics, University of Rajshahi, Rajshahi, Bangladesh, in 2013, 2014, and 2021, respectively. He became a Lecturer and an Assistant Professor with the Statistics Discipline, Khulna University, Khulna, Bangladesh, in September 2018 and November 2020, respectively. Currently, he is a Ph.D. Fellow with the Pattern Processing Laboratory, School of Computer Science and Engineering, The University of Aizu, Japan, under the direct supervision of Dr. Jungpil Shin. He has coauthored more than 45 papers published in widely cited journals and conferences. His research interests include bioinformatics, artificial intelligence, pattern recognition, medical images, signal processing, biomedical data science, machine learning, data mining, and big data analysis.

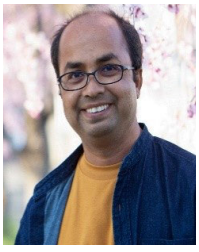

MD. AL MEHEDI HASAN (Member, IEEE) received the B.Sc., M.Sc., and Ph.D. degrees in computer science and engineering from the Department of Computer Science and Engineering, University of Rajshahi, Rajshahi, Bangladesh. He became a Lecturer, an Assistant Professor, an Associate Professor, and a Professor with the Department of Computer Science and Engineering, Rajshahi University of Engineering and Technology (RUET), Rajshahi. He completed a postdoctoral research with the School of Computer Science and Engineering, The University of Aizu, Aizuwakamatsu, Japan. He has coauthored more than 130 publications published in widely cited journals and conferences. His research interests include bioinformatics, artificial intelligence, pattern recognition, medical image, signal processing, machine learning, computer vision, data mining, big data analysis, probabilistic and statistical inference, operating systems, computer networks, and security.

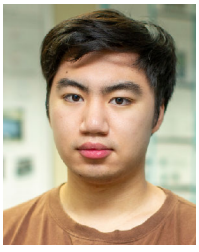

KOKI HIROOKA (Graduate Student Member, IEEE) received the B.Sc. and M.Sc. degrees in computer science and engineering from The University of Aizu (UoA), Japan, in March 2022 and March 2024. Currently, he is a Ph.D. Fellow with the Pattern Processing Laboratory, School of Computer Science and Engineering, UoA, under the direct supervision of Dr. Jungpil Shin. He has coauthored more than six publications published in journals and conferences. His research interests include computer vision, pattern recognition, and deep learning. He is currently working on human activity recognition, human gesture recognition, Parkinson's disease diagnosis, and ADHD diagnosis.

YUKI HAGIHARA received the Medical degree from Ehime University School of Medicine, Japan, in 2018. She is currently pursuing the Ph.D. degree under the guidance of Prof. Shunsuke Kobayashi. She is also enrolled in a Neurology Residency Program with Teikyo University. Her research focuses on neuropsychology and movement disorders.

NAOKI KOTSUKI graduated from the School of Medicine, Kyorin University, in 2015. He is a Neurologist with Kyorin University Hospital, where he is also conducting research on Parkinson's disease as a Graduate Student. He is a member of the Japanese Society of Neurology and the Japanese Society of Clinical Neurophysiology.

SATOMI INOMATA-TERADA received the Medical degree from the School of Medicine, The University of Tokyo, in 1998, and the Ph.D. degree in neuroscience from the Division of Neuroscience, Department of Neurology, Graduate School of Medicine, The University of Tokyo, in 2008. She is a Board-Certificated Neurologist. She is currently a Research Associate with the Department of Medical Physiology, Kyorin University, Tokyo. She has published papers regarding the saccades in neurodegenerative diseases. Her major research interests include the physiology of neurological disorders, neurodegenerative disease especially spinocerebellar degeneration and basal ganglia disease, eye movement, and clinical neurology. She is a member of the Japan Neuroscience Societies, the Japanese Society of Neurology, and the Japanese Society of Clinical Neurophysiology.

YASUO TERAO received the degree from the School of Medicine, The University of Tokyo, in 1989, and the Ph.D. degree from the Graduate School of Medicine, The University of Tokyo, in 1998. After being trained in internal medicine, he has majored in neurology and is a Board-Certified Neurologist. From 1999 to 2001, he was a Postdoctoral Fellow with the Department of Physiology, Umeå University, Sweden, with Prof. Roland S. Johansson. He became a Lecturer of medicine with the Department of Neurology, The University of Tokyo, in 2012; and a Professor of physiology with the Department of Medical Physiology, Kyorin University, in 2016. He has published and coauthored more than 200 research papers in neurophysiological journals of neurology and neurophysiology. As a clinical neurophysiologist, he has been working on clinical studies of neurological patients using saccade recording and eye tracking methodologies and human studies using various electrophysiological techniques, such as transcranial magnetic stimulation and magnetoencephalography. He serves as an Editor for the *Journal of Neurophysiology*, *Journal of Clinical Neurophysiology*, *Neural Plasticity*, and *Frontiers in Psychiatry*.

SHUNSUKE KOBAYASHI received the Medical degree from the School of Medicine, The University of Tokyo, in 1993, and the D.Phil. degree in neuroscience from the Division of Neuroscience, Department of Neurology, Graduate School of Medicine, The University of Tokyo, in 2002. He is a Board-Certified Neurologist. He is currently a Full Professor of neurology with Teikyo University, Tokyo. He has published over a 100 papers with a cumulative impact factor exceeding 250. His research interests include the functioning of the prefrontal cortex, dopamine physiology, and cognitive dysfunction in Parkinson's disease and related disorders. He holds the position of Councilor in various academic societies, including the Japanese Society of Neurology, the Neuropsychology Association of Japan, the Japan Society for Higher Brain Dysfunction, the Movement Disorder Society of Japan, and the Japanese Society of Neurological Therapeutics. Furthermore, he serves as an Editor for *Frontiers in Neuroscience* and several neurology journals.